International Journal of Engineering and Geosciences
https://dergipark.org.tr/en/pub/ijeg
e-ISSN 2548-0960

Climate patterns in Europe: A focus on ten countries through remote sensing

Volkan Yilmaz

Karadeniz Technical University, Department of Geomatics Engineering, Türkiye, volkanyilmaz.jdz@gmail.com

Cite this study: Yilmaz, V. (2025). Climate patterns in Europe: A focus on ten countries through remote sensing. International Journal of Engineering and Geosciences, 10 (3), 398-418.

https://doi.org/10.26833/ijeg.1583206

Keywords
Climate Change
Remote Sensing
Time-series Analysis
Land Surface Temperature
Precipitation

Research Article

Received:11.11.2024
1.Revised: 28.01.2025
2.Revised: 11.03..2025
Accepted:14.03.2025
Published:01.10.2025

Abstract

Leveraging high-temporal resolution remote sensing data enables the investigation of the impacts of climate change with unprecedented detail and accuracy. This approach provides consistent observations, allowing for tracking of short-term fluctuations and long-term trends in climate patterns. The majority of existing studies focus on local impacts, overlooking broader national-scale implications. This research addresses this gap, examining the effects of climate change on European countries, i.e., Türkiye, Germany, Belgium, the United Kingdom (UK), France, Spain, Switzerland, Italy, Ukraine and Poland from 2001 to 2023, emphasizing the interconnected nature of climate change and the need for comprehensive strategies on a national scale. This research involved a comprehensive examination of essential environmental variables, such as precipitation (PCP), land surface temperature (LST), evapotranspiration (ET), potential evapotranspiration (PET), normalized difference vegetation index (NDVI), vegetation condition index (VCI), temperature condition index (TCI), vegetation health index (VHI) and forest area loss (FAL) through an extensive time-series analysis. The primary aim was to reveal temporal patterns within these datasets. Subsequently, pair-wise correlations among the datasets were computed, offering valuable insights into the complex interconnections among the factors used. The experiments revealed that the UK experienced a significant decline in PCP, while Ukraine and Poland exhibited higher rates of LST increase. Switzerland, France and Italy showed higher ET rates; and Belgium, France and Italy exhibited the highest rate of PET increase. Türkiye, Poland and Italy had a more pronounced rise in vegetation health. The study found strong positive correlations (average 0.72) between LST and PET. Additionally, LST showed a notable correlation with NDVI (average 0.55) and VCI (average 0.42). PCP generally exhibited negative correlations with other factors and ET was generally correlated with both NDVI (average 0.55) and VCI (average 0.56). This study is expected to contribute to the understanding of the impacts of climate change on national scale.

1. Introduction

Climate change has become a paramount concern in our era, posing extensive implications for the environment, ecosystems and human communities. While the Earth's climate is naturally dynamic, the acceleration of climate system changes is predominantly attributed to human activities, notably the combustion of fossil fuels and deforestation. Understanding and monitoring these changes are critical for devising effective strategies to mitigate and adapt to the impacts of climate change. Addressing the need to combat climate change and its effects is now recognized as one of the seventeen worldwide Sustainable Development Goals (SDG 13) outlined in the United Nations (UN) Agenda 2030 [1,2]. The data collected through climate monitoring initiatives enable scientists, policymakers and communities to identify trends, assess risks and implement strategies to address the challenges posed by a changing climate.

Key components of climate monitoring include the measurement of land surface temperature (LST) [3-9], evapotranspiration (ET) [10-13], precipitation (PCP) [14] and greenhouse gas concentrations [15,16]. The measurement of LST emerges as a crucial element of climate change, providing valuable insights into the dynamics of Earth's ecosystems. LST influences various ecological processes, such as plant growth, evaporation and heat exchange between the land and the atmosphere. Monitoring changes in LST helps scientists detect alterations in land cover [17], urbanization patterns [18] and the overall health of forest ecosystems [19]. The

phenomenon known as the urban heat island effect, characterized by elevated temperatures in cities compared to the surrounding rural areas, exemplifies how LST measurements play a crucial role in comprehending the human-induced influences on both local and global climates [20]. ET refers to the natural process involving the combined water loss through both evaporation and plant transpiration into the atmosphere [21]. Evaporation converts liquid water from sources like soil, lakes, or rivers into water vapour through solar energy, while transpiration releases water vapour from plants during photosynthesis [22]. This combined water vapour release influences the water cycle and is pivotal in climate regulation. Understanding and measuring ET are integral elements in climate change research [21], offering valuable insights into water availability [23,24] and regional climate dynamics [25,26]. PCP holds a central role in the examination of climate change. Alterations in PCP patterns represent conspicuous and impactful signs of a shifting climate. These modifications affect the frequency, intensity and distribution of PCP, with far-reaching consequences for ecosystems [27], agriculture [28] and water resources [29]. More frequent and intense PCP events can lead to flooding, while prolonged periods of drought result in water scarcity. Measuring greenhouse gas concentrations is a fundamental element in addressing the impacts of climate change [30]. Greenhouse gases, including carbon dioxide and methane, capture and retain heat within the Earth's atmosphere, thereby contributing to the phenomenon of global warming [31]. Human activities, particularly the burning of fossil fuels and deforestation, significantly increase these greenhouse gas levels [32]. Monitoring their concentrations is crucial for assessing the extent of human impact on the climate system. The data obtained from these measurements inform climate models, enabling scientists to predict future climate scenarios [33].

Leveraging remote sensing data significantly streamlines the monitoring of climate change due to its capabilities. The comprehensive coverage provided by satellites orbiting the Earth allows for a global perspective [34], enabling researchers to observe climate variables across vast areas. Moreover, the high temporal resolution of remote sensing data facilitates frequent and consistent observations [35], allowing for the tracking of short-term fluctuations and long-term trends in climate patterns. Some popular satellite missions like Sentinel [36,37], Landsat [38,39] and Moderate Resolution Imaging Spectroradiometer (MODIS) [40,41], an instrument aboard the National Aeronautics and Space Administration (NASA) satellites Terra and Aqua, provide free-to-use satellite imagery that can be used for monitoring the effects of climate change. The availability of historical archives and real-time data from free satellite imagery sources allows for comprehensive and long-term analyses, enabling scientists to detect and quantify the effects of climate change over extended periods. This cost-effective approach not only encourages widespread engagement in climate research but also supports the development of innovative solutions to tackle the challenges posed by climate change. Additionally, remote sensing data can be easily integrated into sophisticated models and simulations [42], enhancing the accuracy of climate predictions.

The benefits provided by remote sensing data have positioned them as the leading information source for current research focusing on the investigation of the effects of climate change [43-49]. Mpandeli et al. [50] employed MODIS-derived Normalised Difference Vegetation Index (NDVI) images to assess the water stress from 2000 to 2019 in the Limpopo Province of South Africa. The findings indicate a significant rise in both the frequency and severity of droughts, a decrease in total rainfall, coupled with rising temperatures, leading to heightened water stress specifically during the summer season. Qu et al. [44] used the MODIS-derived Temperature Condition Index (TCI), Vegetation Condition Index (VCI), Vegetation Health Index (VHI) and NDVI in order to analyse the effects of extreme drought in the Horn of Africa (HOA) between 2000 and 2017. The outcomes of the study revealed a severe and increasing trend of vegetation stress and extreme drought in the HOA over the past decades. The research emphasized the consequences of the 2015-2016 El Niño event, considered one of the most potent in documented history, resulting in severe drought in the area. Javadinejad et al. [51] aimed to analyse the monthly and seasonal variations in methane levels from 2012 to 2018 in North America, utilizing satellite data from GOSAT (Greenhouse Gases Observing Satellite) and MODIS, as well as climatic data including temperature, PCP and humidity. The findings indicated an overall increase in methane concentration during this period. The experiments revealed a positive correlation between the methane gas and LST, and a negative correlation between the methane gas and NDVI and PCP. Pádua et al. [52] used aerial imagery data obtained from an unmanned aerial vehicle (UAV) in order to examine the effects of climate change on a vineyard in Portugal. Vigour maps were created using various methods, and the results showed that maps focusing solely on grapevine vegetation provided an accurate depiction of vineyard variability. The study highlighted the significance of these vigour maps in decision-making processes in viticulture, particularly in association with height and water stress estimation. Park et al. [53] developed a model that utilized the Landsat 8 and Shuttle Radar Topography Mission (SRTM) data for drought prediction in a Korean region covering 12 administrative districts. Bannari and Al-Ali [39] investigated the effects of climate change on the spatiotemporal variations in soil salinity over the past three decades (1987-2017) in Kuwait, employing imagery from Landsat 5, Landsat 7 and Landsat 8 satellites. The study underscores the applicability of a semi-empirical predictive model for multi-temporal analyses, highlights the accuracy of Landsat datasets cross-calibration and emphasizes the notable impact of climate change on soil salinity dynamics in the arid landscape of Kuwait. Orusa and Borgogno Mondino [54] utilized MODIS and Climate Hazards Group InfraRed PCP with Station data (CHIRPS) data to explore the effects of climate change in the Alpine region of the Aosta Valley (Italy). The findings underscore the potential of remote

sensing for monitoring climate change effects on alpine vegetation, emphasizing the importance of considering phenology in relation to other environmental factors for effective technological transfer. Zheng et al. [10] introduced a model to estimate the global ET through the use of remote sensing data obtained from the Global Land Surface Satellite (GLASS), Global Precipitation Measurement (GPM), ICESat (Ice, Cloud and land Elevation Satellite) and MODIS satellite. The model was found to effectively partition total ET into plant transpiration and soil evaporation, aligning with ground isotope measurements. Pareeth and Karimi [55] introduced an approach that estimated ET in Lake Urmia Basin (Iran) using Landsat 7 and Landsat 8 images. The results indicated that the proposed approach effectively reconstructed monthly actual ET dynamics across different agriculture land use types, maintaining high spatial variability. A comparison with Food and Agriculture Organisation (FAO) WAter Productivity through Open-access of Remotely sensed data (WaPOR indicates a strong correlation with an R^2 value of 0.93. The study highlighted the approach's applicability to larger basins, suggesting its potential for extension to other geographical areas. Shah and Patel [49] utilized LST images produced from the Landsat 5, Landsat 7 and Landsat 8 satellites in order to examine the spatial distribution of LST in Surat, Ahmedabad and Delhi (India) between 2000 and 2020. Ahmedabad, a landlocked city, was found to exhibit higher temperatures than Surat, a coastal city. The analysis revealed a strong urban heat island effect in medium-dense built-up areas, with impervious surfaces positively correlated and green spaces negatively correlated with LST.

An in-depth review of existing literature uncovered that the majority of prior research concentrated on exploring the impacts of climate change at local scales. In contrast, there has been a scarcity of studies delving into the effects of climate change on a national scale. Focusing predominantly on the effects of climate change at local scales presents certain disadvantages. Firstly, studies confined to local scales may fail to capture the holistic and interconnected nature of climate change impacts. Climate change manifests itself through a complex web of interactions between various environmental, social and economic factors that transcend localized boundaries. Consequently, an exclusive emphasis on local scales may lead to an incomplete understanding of the broader implications, hindering the development of comprehensive mitigation and adaptation strategies. Secondly, localized studies often lack the ability to discern regional patterns and variations, thereby limiting the generalizability of findings. Climate change is characterized by spatial heterogeneity and its effects may vary significantly across different regions within a country. A singular focus on local scales may overlook critical nuances and trends that are only discernible when analysing a broader geographical scope. This limitation may impede the applicability of research findings to larger areas, potentially hindering the formulation of effective policies that address climate change on a national scale. Moreover, climate change is inherently interconnected with various sectors and its effects may cascade across regions, affecting the overall resilience and sustainability of a country. By concentrating solely on local scales, researchers risk neglecting systemic vulnerabilities that can only be identified through a more comprehensive assessment. On the other hand, as stated by Reiners et al. [3], existing research on examining the effects of climate change at the country scale has predominantly cantered on China and the USA, with limited attention given to European countries. In the light of all these, the objective of this research is to investigate the effects of climate change on European countries, including Türkiye, Germany, Belgium, the United Kingdom (UK), France, Spain, Switzerland, Italy, Ukraine and Poland during the period from 2001 to 2023. These countries encompass a range of climatic zones and agro-ecological conditions, which align with the objective of capturing a broad spectrum of climate trends across the European continent. While the study does not include all European nations, this focused selection was designed to balance feasibility with the need for comprehensive insights into climate variability. The chosen countries represent different agro-climatic regions of Europe, such as the Mediterranean region (e.g., Spain, Italy, and Türkiye), the Oceanic region (e.g., France, the UK, and Belgium), the Continental region (e.g., Germany, Poland, and Ukraine), and the Alpine region (e.g., Switzerland). This classification captures the climatic diversity across Europe, ensuring that trends observed in the study are relevant to distinct environmental, agricultural, and socio-economic contexts. For example, the Mediterranean region is characterized by hot, dry summers and wet winters, making it particularly sensitive to climate change impacts such as drought and heatwaves. Conversely, the Continental and Oceanic regions provide insights into contrasting climatic conditions with varying levels of precipitation, seasonal temperature variation, and agricultural practices.

2. Method

2.1. Study area

As temperatures increase, weather patterns change, and occurrences of extreme events become more frequent, countries find themselves navigating a complex web of challenges and opportunities. From the Mediterranean to the Alps, each country experiences climate change uniquely, shaped by factors such as geographical location, socio-economic structures and policy responses. An in-depth understanding of the nuanced impacts of climate change on European countries is vital for assessing vulnerability and formulating effective strategies for mitigation and adaptation. Hence, this study aimed to investigate the impacts of climate change on European countries Türkiye, Germany, Belgium, the UK, France, Spain, Switzerland, Italy, Ukraine and Poland during the period between 2001 and 2023.

Türkiye's diverse climate zones include Mediterranean (hot, dry summers; mild, rainy winters), Black Sea (cool summers; warm coastal winters; snowy,

cold higher elevations), Continental (significant seasonal and daily temperature variations) and Marmara (transitional with traits of the other climates). Most rainfall occurs in winter and spring, while summer features decreased PCP, higher temperatures and increased evaporation [56].

Germany has a temperate climate with mild temperatures, well-distributed rainfall ideal for agriculture and infrequent extreme temperatures. Rapid climate changes occur due to Atlantic westerly winds meeting cold north eastern air masses. Coastal regions exhibit maritime influences, while eastern and south eastern areas show more continental characteristics [57].

Belgium experiences a temperate maritime climate characterized by mild summers and moderate winters owing to its proximity to the North Sea and Atlantic Ocean. Climate variation is minimal across the country, though maritime effects lessen inland. Rainfall is consistent year-round, with a drier period from April to September. Powerful Atlantic low-pressure systems bring strong winds and adverse weather in autumn and winter, while easterly winds can cause warmer, drier summers and colder winters [58].

The UK's maritime, damp and temperate climate features moderate temperatures and annual PCP between 800 mm and 1400 mm. Influenced by the Atlantic Ocean and the Gulf Stream, the climate varies regionally due to proximity to the Atlantic and topography, with the southeast experiencing more continental influences. Prevailing westerly winds contribute to these regional differences [59].

France's climate is favourable for cultivation, with most of the country in the temperate zone and a subtropical influence in the south. Oceanic influences, moderated by the North Atlantic Drift and Mediterranean Sea, bring rainfall mainly from westerly Atlantic winds. Higher elevations in western and north western France receive over 50 inches (1270 mm) of rain annually. France's climate is divided into oceanic, continental and Mediterranean zones, with variations in the Aquitaine Basin and mountains [60].

Spain's climate is divided into three main zones: Mediterranean (hot, dry summers; mild, rainy winters), central Meseta (hot, dry summers; cold winters with spring and autumn rainfall) and northern maritime (cool summers; mild, frequently rainy winters). Mountainous areas receive higher rainfall and heavy winter snow. The Mediterranean coast has moderate spring and autumn rain, while Murcia experiences an almost African climate. The Atlantic coast has cooler summers and substantial winter rainfall [61].

Switzerland's climate is influenced by four major European air masses: mild, moist western air from the North Atlantic Drift, dry cold air from the Arctic, dry cold eastern continental air in winter and warmer in summer, and warm, moist Mediterranean air. These intersecting air masses create dynamic weather patterns, with local relief causing significant temperature and PCP variations, adding complexity to the climate [62].

Italy has a Mediterranean climate with warm, dry summers and cool, wet winters. Northern and mountainous regions experience cool, humid winters with occasional snow. Coastal areas stay warm due to high sea temperatures, though storms like the Mistral can bring snow and gales. Summers, especially in the south, can be hot with temperatures reaching up to 40°C. Thunderstorms are frequent in the north and Sirocco winds from Africa can bring intense heat. Local climate variations include coastal breezes and cooler mountain regions with afternoon showers [63].

Ukraine's climate varies by region: temperate continental in the north and west with warm summers and cold winters and high PCP (100 rainy days/year). The central and eastern regions experience hotter summers and cold winters, with less PCP. The Carpathian Mountains have a colder mountain climate with more snowfall. Southern Ukraine, influenced by the Black Sea, has a temperate maritime climate with milder temperatures (22°C-27°C in summer, 0°C to 2°C in winter) and higher PCP [64].

Poland's climate is transitional between maritime and continental, with six distinct seasons: snowy winter, variable early spring, sunny spring, warm, rainy summer, sunny autumn and a foggy, humid late autumn. Sunshine peaks over the Baltic in summer and the Carpathians in winter. Annual PCP averages 24 inches (610 mm), higher in the mountains (31 to 47 inches) and lower in the central lowlands (18 inches), with snow contributing significantly in winter [65]. The geographic locations of all countries focused on can be seen in Fig. 1.

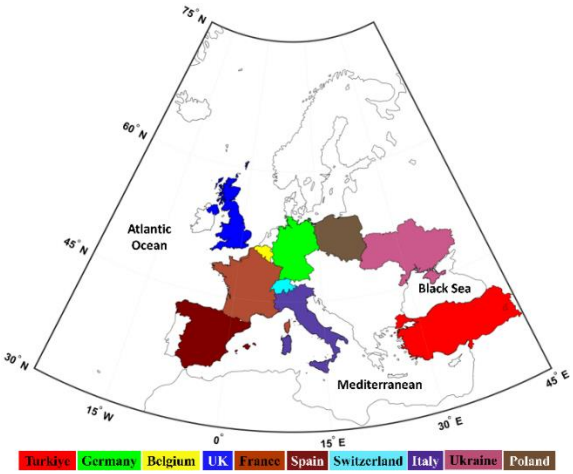

Figure 1. The geographic locations of all countries examined.

2.2. Data used

Time-series analysis of satellite data plays a crucial role in climate change monitoring by providing a continuous and comprehensive perspective on the impacts of climate change over time. Moreover, extended observation periods are crucial for comprehending the influence of both human activities and natural processes on the climate. The insights gained from time-series analysis contribute to the development of precise models for predicting future climate scenarios, aiding policymakers, researchers and the public in making well-informed decisions and implementing effective strategies to address the effects of climate change. Hence,

this study investigated the effects of climate change on the aforementioned countries through time-series analysis of PCP, LST, ET, potential ET (PET), NDVI, forest area loss (FAL) data obtained from the Google Earth Engine (GEE) platform; as well as the time-series analysis of TCI, VCI and VHI data computed. These parameters were chosen for their ability to comprehensively capture the effects of climate change on ecosystems, vegetation, and water resources. Climatic variables like PCP and LST provide insights into temperature and precipitation changes, while ET and PET assess water fluxes and stress. Indices like NDVI, VCI, TCI, and VHI monitor vegetation health, productivity, and resilience to climatic stressors such as drought or heatwaves. FAL tracks forest ecosystem degradation, critical for understanding the impacts of climate change on biodiversity and carbon sequestration. These parameters, combined with the availability of high-quality remote sensing data, allow for a thorough examination of climate change effects across Europe's diverse landscapes.

2.2.1. PCP data

This study conducted the time-series analysis of PCP using CHIRPS dataset (collection ID: UCSB-CHG/CHIRPS/DAILY) obtained from the GEE. CHIRPS represents a rainfall dataset spanning over 30 years on a quasi-global scale [66]. Utilizing 0.05° resolution satellite imagery along with in-situ station data, CHIRPS generates gridded time series of rainfall, enabling trend analysis and seasonal drought monitoring. CHIRPS dataset is highly valuable for offering rainfall estimation data in regions lacking rain gauges [67]. The dataset provides PCP data for the period between 1981 and July 2024 [68].

2.2.2. LST data

The time-series analysis of LST was carried out using MOD11A1.061 dataset (collection ID: MODIS/061/MOD11A1) obtained from the GEE. The dataset, generated by NASA LP DAAC (Land Processes Distributed Active Archive Centre) at the USGS (United States Geological Survey) EROS (Earth Resources Observation and Science) Centre, provides daily information on LST and emissivity in grids with a size of 1200 x 1200 km. This MODIS-derived dataset encompasses LST information spanning the years 2000 to present day [69].

2.2.3. ET and PET data

The time-series analysis of ET and PET were carried out using MOD16A2.061 dataset (collection ID: MODIS/061/MOD16A2) generated by the NASA LP DAAC at the USGS EROS Centre and distributed through the GEE platform. The dataset is a composite product spanning eight days and generated at a resolution of 500 m per pixel. The values assigned to the pixels in the evapotranspiration bands (i.e., ET and PET) represent the cumulative sum of data from all eight days during the composite period. The dataset provides ET and PET data for the period between 2001 and July 2024 [70].

2.2.4. NDVI data

The examination of vegetation condition through time-series analysis utilized MOD13Q1.061 NDVI dataset (collection ID: MODIS/061/MOD13Q1), which was produced by the NASA LP DAAC at the USGS EROS Centre and made available via the GEE platform. This MODIS-derived dataset provides 16-day composite vegetation information for the period between 2000 and July 2024 [71].

2.2.5. VCI data

VCI, a pixel-wise normalization of NDVI, proves valuable for conducting relative evaluations, specifically at the pixel level. It effectively filters out the impact of local geographic resources on the spatial variability of NDVI, allowing for more precise assessment of changes in NDVI [72]. VCI exhibits sensitivity to drought, capable of mitigating the influence of not only geographical location, but also ecological systems and soil conditions on NDVI. This characteristic renders it an excellent indicator for monitoring drought on a large scale [73,74]. VCI varies from 0% to 100%, where lower VCI values refer to poorer vegetation growth and increased levels of drought. VCI index is computed as [72];

$$VCI_{ijk} = \frac{NDVI_{ijk} - NDVI_{i,min}}{NDVI_{i,max} - NDVI_{i,min}} \times 100 \quad (1)$$

where, $NDVI_{ijk}$ is the monthly NDVI value for pixel i in the j^{th} month of year k. $NDVI_{i,min}$ and $NDVI_{i,max}$ denote the multiyear minimum and maximum NDVI value for the pixel i in the j^{th} month, respectively. NDVI values were obtained from MOD13Q1.061 NDVI dataset [71].

2.2.6. TCI data

TCI is used to assess water stress in vegetation caused by temperature and has been extensively utilized to observe current drought conditions [75-78]. TCI values may range from 0%, indicating adverse conditions, to 100%, representing optimal conditions. TCI is calculated as [79,80];

$$TCI = \frac{LST_{max} - LST_{current}}{LST_{max} - LST_{min}} \times 100 \quad (2)$$

where, $LST_{current}$ represents the day-specific LST being examined in a month, while LST_{min} and LST_{max} denote the monthly lowest and highest LST values observed, respectively. LST values were obtained from the MOD11A1.061 dataset [69].

2.2.7. VHI data

VHI is a composite index used to assess the overall health and condition of vegetation. It is derived from satellite data and integrates multiple indicators to provide a comprehensive view of vegetation health over large geographic areas. VHI is calculated as [79];

$$VHI = \alpha VCI + (1 - \alpha)TCI \quad (3)$$

Table 1. Characteristics of the GEE catalogue data used for time series analysis.

Description	Unit	Min	Max	Scale	Date range	Resolution
PCP	mm/day	0	1444.34	--	01/01/2001 - 12/31/2023	5566 m
LST	K	7500	65535	0.02	01/01/2001 - 12/31/2023	1000 m
ET	kg/m^2/8day	-32767	32700	0.1	01/01/2001 - 12/31/2022	500 m
PET	kg/m^2/8day	-32767	32700	0.1	01/01/2001 - 12/31/2022	500 m
NDVI	--	-2000	10000	0.0001	01/01/2001 - 12/31/2022	250 m
FAL	--	--	--	--	01/01/2001 - 12/31/2023	30.92 m

where, α specifies the relative contributions of VCI and TCI. Due to the absence of precise information, a value of 0.5 is generally assigned to α, assuming that both variables contribute equally to the combined index [81,82]. VHI values close to 100% indicate good vegetation health, with optimal growing conditions; while values close to 0% indicate poor vegetation health, possibly due to drought, heat stress, or other adverse conditions.

2.2.8. FAL data

The time-series analysis of FAL was carried out using the Hansen Global Forest Change v1.11 dataset (collection ID: UMD/hansen/global_forest_change_2023_v1_11) [83], which is distributed through the GEE platform [84]. The dataset offers information on tree cover, forest area gain, FAL and the annual rate of forest loss at a 30-m spatial resolution. The accuracy of this dataset may differ across regions due to distinct change dynamics and data availability challenges [85].

The characteristics of the GEE catalogue data used for the time series analysis are outlined in Table 1. As shown, data for PCP, LST and FAL were available from 01/01/2001 to 12/31/2023, which allowed for the calculation of TCI data for the same period. Although the GEE data catalogue indicates that ET/PET and NDVI data are available from 01/01/2001 to 07/11/2024 and from 02/18/2000 to 07/11/2024, respectively, it was not possible to retrieve all the data for these periods. Therefore, ET, PET and NDVI data were collected for the period from 01/01/2001 to 12/31/2022, enabling the calculation of VCI and VHI data for the same period.

2.2.9. Population data

This research also explored how population (PPL) trend influenced the factors employed in evaluating the consequences of climate change, with a specific focus on each country. Yearly PPL data for all countries, excluding Türkiye, was sourced from [86]. For Türkiye, the PPL information was retrieved from the official website of the Turkish Statistical Institute [87].

2.3. Methodology

In this study, an extensive time-series analysis was undertaken on key environmental parameters, including PCP, LST, ET, PET, NDVI, VCI, TCI, VHI and FAL. The primary objective was to unveil temporal trends within these datasets. Following this analysis, Mann-Kendall test [88,89] was applied to see if the trends were statistically significant. Since this test does not provide information about the magnitude of trends [90], pair-wise Pearson correlation coefficient (significance level: 0.05) was calculated between datasets, providing valuable insights into the intricate relationships among the factors utilized in evaluating the repercussions of climate change. Although the majority of the datasets extended their records until the year 2024, this study opted to focus on the period spanning from January 2001 to December 2022. This decision was influenced by the aforementioned temporal limitation of ET, PET and NDVI data. By concentrating on this specific timeframe, the research aims to ensure consistency across the datasets, enabling a comprehensive examination of the dynamics between these environmental variables and their implications for the assessment of the impacts of climate change. The correlation analysis also investigated whether the rise in PPL had any influence on the investigated environmental factors.

3. Results and discussion

3.1. Trend analysis

The regression lines derived from the time-series analysis of environmental parameters for each country were generated with the aim to reveal the discernible trends within these datasets. Fig. 2 displays the trend lines obtained through the time-series analysis of annual total PCP, annual average LST, annual total ET, annual total PET, annual average NDVI, annual average VCI, annual average TCI, annual average VHI, annual total FAL and annual total PPL values for each country. Table 2 presents the linear regression equations of trend lines in order to better interpret the trends.

As seen in Table 2, all countries experienced a decrease in total annual PCP between 2001 and 2023. The UK stands out with a particularly significant negative trend, signalling a substantial decline in PCP. Even in the UK, renowned for its excess PCP, the decrease in total PCP reveals the adverse effects of climate change. Belgium and Italy experienced the most rapid declines in annual total PCP after the UK, which could have significant implications for water resources, agriculture and ecosystem stability. Countries like France, Germany and Switzerland showed moderate declines, indicating potential but less dramatic impacts. Türkiye, Spain, Ukraine and Poland showed slower rates of decline, suggesting more gradual changes in their PCP patterns. The observed decline in PCP across European countries can be attributed to altered atmospheric circulation patterns resulting from global climate change. As the Earth's average temperature rises due to increased greenhouse gas concentrations, atmospheric dynamics shift, affecting regional PCP patterns. Specifically, the warming of the atmosphere influences the movement

and intensity of weather systems, often leading to reduced PCP in some areas while increasing the frequency of extreme rainfall events in others.

Table 2 shows that all countries have positive slopes in their regression equations, indicating a general increase in annual average LST between 2001 and 2023. This trend is consistent with global warming and indicates a warming climate. Ukraine and Poland experienced the most rapid increases in annual average LST, suggesting these regions are undergoing significant climatic changes that could have various impacts on their environments and economies. Germany, Belgium, Switzerland and France showed moderate rates of LST increase. Türkiye, Spain, Italy and the UK exhibited slower rates of LST increase, suggesting more gradual changes in their climate, though still indicative of overall warming. It should be noted that rising greenhouse gas emissions, primarily from fossil fuel combustion, deforestation, and industrial activities, enhance the greenhouse effect, trapping more heat in the Earth's atmosphere. This warming is not uniform, with varying rates of temperature increase across different regions. The observed rise in LST contributes to more frequent heatwaves, and alters local climatic conditions, further influencing PCP patterns and evaporation rates.

The regression line equations given in Table 2 depict that total annual ET increased in all countries between 2001 and 2022. Switzerland, France, Italy and Poland showed the highest increases in ET, indicating significant climatic impacts leading to higher water transfer from land surfaces. Türkiye, Spain, the UK, Ukraine and Germany exhibited moderate increases, reflecting steady climatic influences on ET. Belgium showed the lowest rate of increase, suggesting slower climatic changes affecting ET. The countries with significant increases in annual average LST (e.g., Ukraine, Poland, Germany) also exhibited notable increases in ET. This is expected as higher temperatures typically enhance the rate of evaporation and transpiration. On the other hand, the general decline in annual total PCP observed across these countries suggests that less water is available, yet the increase in LST and ET indicates that the water that is available is being lost more quickly to the atmosphere. This could exacerbate water scarcity issues. As seen from the experiments, the rate of LST increase and ET varies by region, with some countries like Switzerland and France showing high rates of both, while others like Belgium show more gradual changes.

As seen in Table 2, all countries have positive slopes in PET regression equations, indicating an increasing trend in PET between 2001 and 2022. This is consistent with rising temperatures and changing climatic conditions. Belgium, France, Italy and Germany showed the highest rates of increase in PET during this time period, suggesting these countries are experiencing more significant climatic changes, leading to higher potential water demand. Switzerland, Spain, the UK and Poland exhibited moderate increases in PET, indicating substantial but less extreme changes. Ukraine and Türkiye showed the slowest increase in PET, though it still indicates a trend towards higher potential water demand. Countries experiencing declining annual total PCP will likely face more significant challenges as increasing PET combined with less PCP can lead to water shortages and stress on water resources. The increase in PET, often outpacing the rise in ET as in this study, suggests that the capacity of the atmosphere to absorb moisture is growing faster than the actual moisture return to the atmosphere through PCP. This imbalance results in greater moisture deficits and can lead to soil desiccation, increased drought stress, and diminished agricultural productivity. The disparity between PET and ET is particularly pronounced in regions experiencing reduced PCP. As the atmosphere warms, its ability to hold and demand more moisture increases, leading to higher PET values, as in the European countries studied. However, if PCP does not keep pace with this demand, the result is a heightened water deficit. This discrepancy underscores the growing challenge of managing water resources, as regions may experience more frequent drought conditions, impacting natural ecosystems.

Table 2 shows that all countries indicated a general increase in NDVI values between 2001 and 2022. This suggests an improvement in vegetation health or density across these countries. Poland exhibited the highest rate of increase in NDVI, suggesting significant improvements in vegetation health or density over time. Türkiye, Germany, France, Switzerland and Italy showed moderate increases, indicating steady improvements in vegetation conditions. Belgium, the UK and Ukraine showed slower increases, leading to more gradual improvements in vegetation health. Countries with significant increases in annual average LST might also experience changes in vegetation growth patterns. Higher temperatures can enhance plant growth in temperate regions but may stress vegetation in already warm areas. Declining PCP trends, as observed in all countries, can stress vegetation and potentially counteract NDVI increases. Countries with moderate PCP decreases and significant NDVI increases (e.g., France, Germany, Italy) might be adopting effective water management and conservation practices. Countries with high ET increases and moderate NDVI growth (e.g., Italy, Spain) suggest that despite higher water demand, vegetation health is improving, possibly due to effective irrigation and agricultural practices.

As seen in Table 2, all countries have negative slopes in TCI regression equations, indicating a general decrease in TCI values over time. This suggests that temperature conditions became less favourable for vegetation and ecological health between 2001 and 2023. Switzerland, Belgium, Germany and France showed the most significant decreases in TCI, indicating rapidly worsening temperature conditions for vegetation. The UK, Poland and Ukraine exhibited moderate declines, suggesting steady but less severe worsening conditions. Spain, Türkiye and Italy experienced the least decreases in TCI, indicating more gradual changes in temperature conditions. Rising ET rates indicate higher water loss, which, combined with decreasing TCI, suggests increasing stress on vegetation due to unfavourable temperature conditions and water scarcity.

Table 2. Linear regression equations of trend lines for all climate variables.

Country	PCP	LST	ET	PET
Türkiye	y = -1.846x + 644.74	y = 0.026x + 20.75	y = 1.9509x + 308.20	y = 2.9666x + 1442.60
Germany	y = -4.6891x + 918.85	y = 0.0825x + 12.81	y = 1.5268x + 372.29	y = 4.0004x + 702.52
Belgium	y = -8.7279x + 985.70	y = 0.0814x + 13.91	y = 0.4878x + 368.51	y = 4.8153x + 625.50
UK	y = -42.464x + 1535.70	y = 0.0467x + 11.71	y = 1.8937x + 283.32	y = 3.879x + 428.22
France	y = -4.2422x + 888.07	y = 0.0654x + 16.01	y = 2.8591x + 436.29	y = 4.8x + 855.51
Spain	y = -2.9571x + 676.47	y = 0.0394x + 22.20	y = 1.9033x + 325.26	y = 3.6497x + 1361.10
Switzerland	y = -3.1154x + 1317.00	y = 0.0712x + 9.43	y = 2.9972x + 427.22	y = 3.989x + 799.73
Italy	y = -4.8858x + 892.59	y = 0.0389x + 18.71	y = 2.7009x + 476.25	y = 4.853x + 1201.90
Ukraine	y = -2.2621x + 612.91	y = 0.1011x + 13.97	y = 1.6221x + 392.25	y = 1.0932x + 955.65
Poland	y = -3.1021x + 824.56	y = 0.0922x + 11.67	y = 2.5953x + 359.08	y = 3.1021x + 734.79
Country	**NDVI**	**TCI**	**VCI**	**VHI**
Türkiye	y = 0.003x + 0.31	y = -0.026x + 37.12	y = 0.3876x + 46.16	y = 0.1792x + 41.65
Germany	y = 0.0029x + 0.54	y = -0.1721x + 41.37	y = 0.2702x + 65.12	y = 0.0548x + 53.20
Belgium	y = 0.0018x + 0.58	y = -0.1841x + 42.29	y = 0.1927x + 67.12	y = 0.0218x + 54.56
UK	y = 0.0015x + 0.58	y = -0.1257x + 43.55	y = 0.1752x + 65.39	y = 0.0313x + 54.42
France	y = 0.002x + 0.58	y = -0.1459x + 43.44	y = 0.2709x + 63.88	y = 0.0719x + 53.59
Spain	y = 0.002x + 0.43	y = -0.0321x + 41.79	y = 0.3169x + 48.31	y = 0.145x + 45.03
Switzerland	y = 0.0025x + 0.41	y = -0.1924x + 42.35	y = 0.1805x + 57.45	y = -0.0042x + 49.88
Italy	y = 0.0028x + 0.50	y = -0.0194x + 40.07	y = 0.4037x + 56.37	y = 0.192x + 48.22
Ukraine	y = 0.0014x + 0.41	y = -0.0976x + 36.04	y = 0.0638x + 52.76	y = -0.0335x + 44.53
Poland	y = 0.0043x + 0.47	y = -0.111x + 37.22	y = 0.3998x + 60.19	y = 0.1374x + 48.76
Country	**FAL**	**PPL**		
Türkiye	y = 952.98x + 11511	y = 963394x + 6E+07		
Germany	y = 3959.8x + 2091.4	y = 111843x + 8E+07		
Belgium	y = 103.27x + 3034.8	y = 67315x + 1E+07		
UK	y = 392.96x + 14975	y = 428868x + 6E+07		
France	y = 1294.6x + 37212	y = 269193x + 6E+07		
Spain	y = 2261.9x + 24820	y = 259232x + 4E+07		
Switzerland	y = 61.929x + 1082.9	y = 77613x + 7E+06		
Italy	y = 1271.4x + 2257.9	y = 100566x + 6E+07		
Ukraine	y = 1130.8x + 29865	y = -319671x + 5E+07		
Poland	y = 1636.2x + 27579	y = 32842x + 4E+07		

Table 2 depicts that all countries experienced increase in annual average VCI values between 2001 and 2022, indicating that vegetation conditions improved in this period. Italy, Poland and Türkiye showed the most significant increases in VCI, indicating more considerable improvements in vegetation health, compared to the other countries. Spain, France, Germany and Belgium exhibited moderate increases, suggesting steady but less dramatic improvements in vegetation health. Switzerland, the UK and Ukraine showed the least increases in VCI values. This might reflect stable but slowly improving conditions or lesser emphasis on vegetation management, compared to the other countries. Rising temperatures can stress vegetation, but countries with increasing VCI may have adapted through heat-resistant crops or improved agricultural practices. For example, Italy and Spain showed significant VCI improvements despite warmer climates. As for VHI, all countries except for Switzerland and Ukraine showed an increase in annual average VHI values between 2001 and 2022, which can be seen in Table 2. Italy, Türkiye, Spain and Poland showed the most significant increases in VHI, indicating considerable improvements in vegetation health. France and Germany exhibit moderate increases whereas the UK and Belgium experienced the least increases. The countries with significant improvements in VCI also tend to show improvements in VHI (e.g., Italy, Türkiye, Poland), as both indices measure aspects of vegetation health. This consistency reinforces the reliability of the observed trends.

Table 2 shows that all countries experienced an increase in FAL between 2001 and 2023. The regression equations show that Germany, Spain and Poland have the steepest slopes, suggesting these countries experienced the most rapid increases in FAL in this period. This trend could be driven by various factors such as increased agricultural expansion, urbanization and logging activities. On the other hand, France, the UK, Ukraine and Poland have high intercepts, indicating significant initial deforestation, which suggests that these countries have longstanding deforestation issues that are continuing to worsen. Switzerland and Belgium have the lowest slopes, indicating slower rates of increase in FAL. The trends in FAL can be related to changes in PCP, LST and ET. Regions with worsening climatic conditions (e.g., Germany, France) might see accelerated deforestation due to increased vulnerability of forests to fires, pests and diseases. Fig. 3 shows the temporal trends of PCP in France, LST in Ukraine, ET in Switzerland, and NDVI in Poland between 2001 and 2023. The reason for showing only the temporal trends in these countries is because they exhibited a relatively greater amount of change in the examined climate parameters.

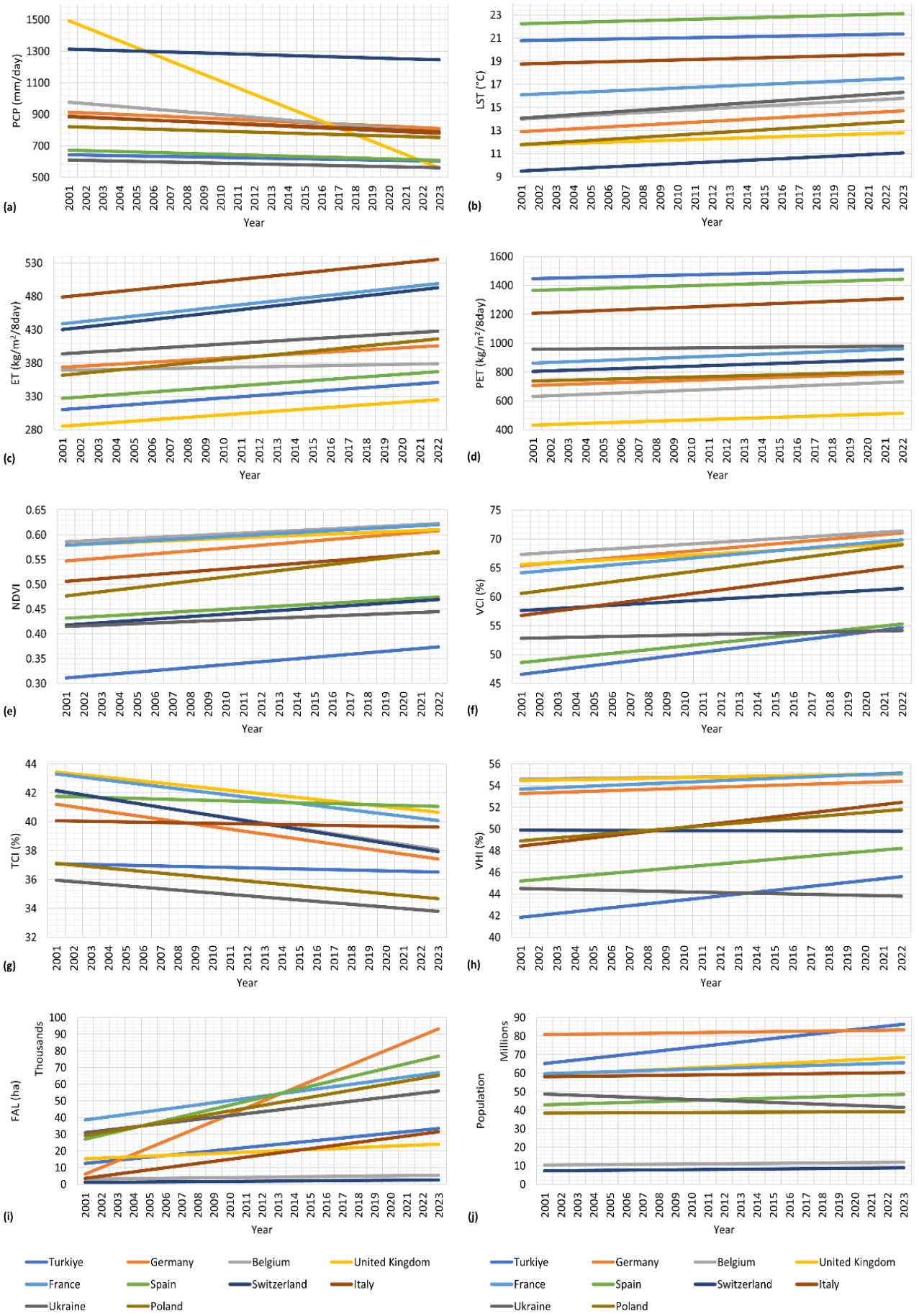

Figure 2. Trend lines obtained through the time-series analysis of annual total PCP (a), annual average LST (b), annual total ET (c), annual total PET (d), annual average NDVI (e), annual average VCI (f), annual average TCI (g), annual average VHI (h), annual total FAL (i) and annual total PPL (j).

As seen in Table 2, all countries except for Ukraine experienced PPL increase between 2001 and 2023. The PPL of Türkiye and the UK showed the most rapid growth in this period. From 2001 to 2023, the PPL in Türkiye, Switzerland, Spain, the UK, Belgium, France, Poland, Italy and Germany increased by approximately 30%, 22%, 16%, 15%, 13%, 10%, 6%, 3% and 2%, respectively. Ukraine's PPL declined by about 24%. The ongoing conflict in Ukraine has undeniably been a major factor in this reduction over the past two years. PPL growth can exacerbate deforestation, increase pressure on natural resources and contribute to higher levels of pollution. Countries with rapid PPL growth, such as Türkiye and the UK, may need to implement stringent environmental protection measures to mitigate these impacts. Increased PPL can also affect vegetation health and climate indices. More people can lead to more land being used for housing and agriculture, potentially decreasing VCI and VHI. It is crucial to take immediate measures to protect these indices while they are still showing positive trends.

3.2. Mann-Kendall test results

Table 3 shows the Z-scores calculated within the Mann-Kendall test, which is a popular tool used to identify the significance of trends. Typically, a Z-score needs to be beyond the critical value of ±1.96 to be considered significant at the commonly used 0.05 significance level. As seen in Table 3, Türkiye, France, Spain, Switzerland, Italy, Ukraine and Poland exhibited decreasing trends in PCP between 2001 and 2023, with Z-scores ranging from -0.96 to -1.58. However, these trends are not statistically significant, suggesting that the observed decreases could be due to natural variability rather than a persistent trend. Conversely, Germany, Belgium and the UK showed significant decreasing trends in PCP. These significant Z-scores indicate a notable decline in PCP, highlighting the potential for increased drought risk and water scarcity in these regions. Table 3 also depicts that all countries except Spain (1.41) and Italy (1.80) showed statistically significant increasing trends in LST between 2001 and 2023, with Z-scores above the critical value of 1.96. These findings underscore the pervasive impact of climate change, with rising temperatures contributing to heatwaves, altered growing seasons and increased ET. The significant warming across most of these countries aligns with global temperature rise patterns, reinforcing the need for robust climate mitigation and adaptation strategies. As also seen in Table 3, between 2001 and 2022, significant increasing trends in ET were observed in all countries except Belgium, which showed a positive but not statistically significant trend. On the other hand, Belgium, the UK, France and Italy experienced considerable increasing trends in PET between 2001 and 2022. The other countries showed statistically insignificant positive trends in PET. These trends indicate an overall increase in atmospheric demand for moisture, driven by rising temperatures, especially in the UK, France and Italy. All countries except Belgium showed significant increasing trends in NDVI, indicating improved vegetation health between 2001 and 2022. This finding is in almost perfect agreement with the Z-scores obtained for VCI data. Table 3 shows that, all countries exhibited negative trends in TCI, indicating worsening temperature conditions. Germany, Belgium, the UK, France, Switzerland, Italy, Ukraine and Poland all showed significant declines between 2001 and 2023. The negative TCI trends reflect increasing temperature stress on ecosystems and agriculture, exacerbating the impacts of rising temperatures and altering growing conditions. All countries except for Belgium and Ukraine were found to show significant increasing trends in VCI between 2001 and 2022. VHI trends were found to be significantly increasing in Türkiye, Italy and Poland, indicating overall improved vegetation health. Germany, the UK, France, Spain and Switzerland showed positive insignificant VHI trends, while Belgium and Ukraine exhibited negative insignificant trends. These trends suggest that despite challenges like increased temperature and ET, vegetation health is improving in many regions, potentially due to adaptation strategies or natural resilience. However, the mixed results highlight the complexity of ecosystem responses to climate variables. As seen in Table 3, FAL trends were significant in Türkiye, France, Spain, Italy, Ukraine and Poland between 2001 and 2023; indicating substantial deforestation. Germany, Belgium, the UK and Switzerland exhibited statistically insignificant positive FAL trends. Deforestation poses significant ecological risks, including loss of biodiversity, increased carbon emissions and altered hydrological cycles. The positive FAL trends for all countries highlight the need for effective forest conservation and reforestation efforts. Table 3 also shows that all countries except for Ukraine and Poland experienced a notable increasing trend in PPL between 2001 and 2023.

3.3. Pair-wise correlation analysis

The pair-wise Pearson correlation coefficients among the datasets were calculated to reveal the relationships between the climate variables focused. Table 4 presents the pair-wise correlation coefficients computed for the variables utilized to evaluate the influences of climate change on Türkiye, Germany, Belgium, the UK and France; whereas Table 5 showcases the pair-wise correlation coefficients computed for Spain, Switzerland, Italy, Ukraine and Poland.

As seen in Tables 4 and 5, in Türkiye, the relationship between PCP and other climate variables reveals some intriguing patterns. There is a weak negative correlation between PCP and LST and PET, which indicates that increases in PCP do not significantly affect surface temperatures or PET rates. However, LST has a strong positive correlation with PET and a weak positive correlation with NDVI, indicating that higher temperatures may promote vegetation growth, as reflected in the NDVI values. ET shows a strong positive correlation with NDVI and the VCI. Notably, ET also has a very strong positive correlation with the VHI. VHI is highly correlated with VCI and NDVI, indicating a strong interdependence among these indices. PPL in Türkiye has strong positive correlations with NDVI, VCI and VHI.

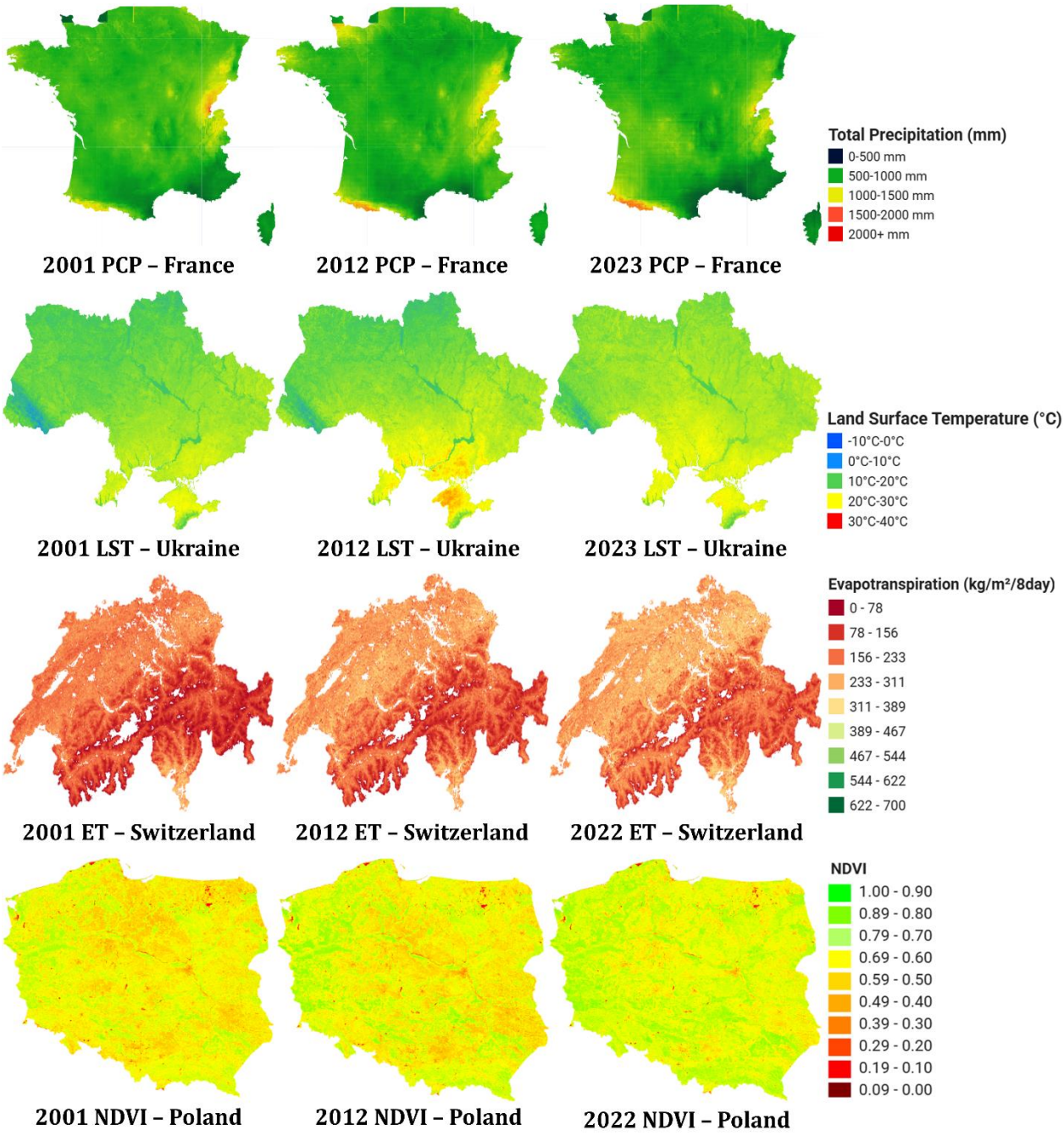

Figure 3. Temporal trends of PCP in France, LST in Ukraine, ET in Switzerland, and NDVI in Poland between 2001 and 2023.

Table 3. Z-scores calculated with the Mann-Kendall test for all climate variables.

Country	PCP	LST	ET	PET	NDVI	TCI	VCI	VHI	FAL	PPL
Türkiye	-1.58	2.09	2.88	1.86	4.00	-1.47	4.29	3.50	2.99	6.49
Germany	-2.09	2.48	2.03	1.80	2.88	-2.37	3.16	1.07	1.92	4.57
Belgium	-2.76	2.59	1.07	2.03	1.89	-2.31	1.64	-0.51	1.47	6.49
UK	-4.57	2.26	2.48	2.54	2.40	-2.03	2.48	0.68	1.58	6.49
France	-1.58	2.31	4.12	2.26	3.47	-1.97	3.44	0.85	2.03	6.49
Spain	-0.96	1.41	2.31	1.58	3.86	-1.41	3.83	1.64	3.89	5.47
Switzerland	-0.96	2.20	2.93	1.86	2.00	-2.26	3.21	1.86	1.52	6.49
Italy	-1.02	1.80	3.44	2.20	4.46	-2.26	4.68	2.76	4.17	2.82
Ukraine	-1.47	2.59	2.37	0.68	2.20	-2.65	1.52	-1.18	2.43	-6.49
Poland	-1.18	2.37	2.82	1.80	3.36	-1.97	4.00	2.54	2.93	-2.71
Significant positive trend						Significant negative trend			No significant trend	

Germany presents a different set of relationships. PCP has a moderate negative correlation with LST, a negative strong correlation with PET and a weak negative correlation with ET. This indicates that higher PCP tends to lower both surface temperatures and ET rates. LST is positively correlated with ET and PET, suggesting that higher temperatures increase both actual and potential ET. NDVI has a strong positive correlation with LST and a weak correlation with ET. The observed positive correlation between NDVI and LST suggests that vegetation growth is associated with warmer conditions. However, this relationship is complex and may be influenced by other factors [91,92], such as water availability, soil type, irrigation, and the presence of snow or waterbodies, which can modulate both NDVI and LST. While temperature is a key factor in vegetation growth, the positive correlation may reflect local environmental or seasonal conditions rather than a direct causal relationship. The TCI has a negative correlation with LST, ET and PET, highlighting the adverse effects of temperature stress on vegetation. VCI is highly correlated with NDVI and moderately with LST. PPL shows a positive correlation with LST, NDVI and VCI.

In Belgium, PCP shows strong negative correlations with LST, ET and PET. LST has strong positive correlations with PET and strong with ET. NDVI is positively correlated with LST and shows a strong correlation with VCI. TCI has strong negative correlations with LST, ET and PET, indicating significant temperature stress impacts on vegetation. VCI is very highly correlated with NDVI, while VHI has a moderate correlation with NDVI. PPL shows moderate positive correlations with LST, NDVI and VCI.

In the UK, PCP has a negative correlation with LST, ET and PET. LST is strongly correlated with ET and PET, indicating that higher temperatures drive higher ET rates. NDVI shows a strong positive correlation with LST and moderate with ET, suggesting that temperature influences vegetation growth. TCI has a very strong negative correlation with LST, indicating significant temperature stress impacts on vegetation. VCI is very highly correlated with NDVI and moderately with LST. PPL shows a very strong negative correlation with PCP and moderate positive correlations with LST and VCI.

In France, PCP has strong negative correlations with LST and PET and a moderate negative correlation with ET. LST shows strong positive correlations with PET and ET. NDVI is positively correlated with LST and ET, indicating that temperature and ET significantly influence vegetation growth. TCI has strong negative correlations with LST, PET and ET, indicating temperature stress impacts. VCI is very highly correlated with NDVI and moderately with LST. PPL shows positive correlations with LST, ET and NDVI. This indicates that France's vegetation health is significantly influenced by temperature and ET.

Spain shows a strong negative correlation between PCP and LST and PET. LST is positively correlated with PET, indicating that higher temperatures increase PET. NDVI has a very strong positive correlation with ET and VCI, suggesting that ET is crucial for vegetation health. TCI has strong negative correlations with LST and PET, indicating temperature stress impacts. VHI is very highly correlated with NDVI and VCI. PPL shows moderate positive correlations with ET, NDVI and VCI.

In Switzerland, PCP has negative correlations with LST, PET and ET. LST is strongly correlated with PET and ET, indicating that higher temperatures increase both potential and actual ET. NDVI has very strong positive correlations with LST and a strong positive correlation with ET. TCI has strong negative correlations with LST and ET. VCI is very highly correlated with NDVI and LST. PPL shows positive correlations with LST, ET and NDVI.

In Italy, PCP shows a strong negative correlation with LST and PET. LST has a strong positive correlation with PET. NDVI is very highly correlated with ET and VCI, indicating the importance of ET on vegetation health. TCI has a strong negative correlation with LST. VHI is highly correlated with NDVI and VCI. PPL shows moderate positive correlations with ET and NDVI.

In Ukraine, PCP has a strong negative correlation with LST. LST is moderately correlated with PET. NDVI has a strong positive correlation with LST, indicating that temperature plays a significant role in vegetation growth. TCI has strong negative correlations with LST and PET, indicating temperature stress impacts. VCI is strongly correlated with NDVI. PPL shows a negative correlation with LST and NDVI. This suggests that Ukraine's vegetation health is significantly influenced by temperature.

In Poland, PCP has weak negative correlations with LST and PET. LST is strongly correlated with PET and moderately with ET. NDVI has very strong positive correlations with LST and moderate with ET, indicating that temperature influences vegetation growth. TCI has strong negative correlations with LST and PET. VCI is highly correlated with NDVI. PPL shows weak correlations with most variables, indicating less influence of these climate variables on PPL trends in Poland.

Due to the differences in climates and geographical conditions of the countries under investigation, it is not possible to definitively establish the relationships between the examined environmental variables. Temperature variables, particularly LST, play a crucial role in influencing vegetation health indices (NDVI, VCI, VHI) across all countries. Negative correlations between PCP and LST are common, indicating that increased temperatures often coincide with reduced PCP. It is challenging to directly link TCI and FAL parameters with other environmental factors. However, it can be noted that PPL increases typically lead to greater FAL in various countries, especially in Türkiye, Germany and Spain. ET and PET are significantly correlated with vegetation indices, emphasizing their importance in vegetation health. PPL shows varying degrees of correlation with climate variables, with some countries like Türkiye and Germany displaying strong links to temperature and vegetation indices, while others like Poland show weaker associations. The findings underscore the critical impact of LST and ET on vegetation health and highlight the complex interplay between climate variables and PPL trends across different regions.

Table 4. Pair-wise correlation coefficients computed for Türkiye, Germany, Belgium, the UK and France.

Country	Data	PCP	LST	ET	PET	NDVI	TCI	VCI	VHI	FAL	PPL
Türkiye	PCP	1.00									
	LST	-0.03	1.00								
	ET	0.13	-0.16	1.00							
	PET	-0.24	0.63	0.11	1.00						
	NDVI	0.10	0.36	0.77	0.31	1.00					
	TCI	-0.32	-0.63	0.26	-0.33	-0.11	1.00				
	VCI	0.07	0.27	0.80	0.30	0.97	-0.07	1.00			
	VHI	-0.07	-0.03	0.86	0.13	0.85	0.37	0.90	1.00		
	FAL	-0.31	0.28	0.11	0.24	0.34	-0.05	0.41	0.36	1.00	
	PPL	-0.23	0.33	0.63	0.41	0.81	-0.14	0.86	0.74	0.63	1.00
Germany	PCP	1.00									
	LST	-0.51	1.00								
	ET	-0.32	0.63	1.00							
	PET	-0.64	0.75	0.81	1.00						
	NDVI	-0.15	0.75	0.38	0.25	1.00					
	TCI	0.51	-0.82	-0.66	-0.86	-0.43	1.00				
	VCI	-0.10	0.56	0.35	0.13	0.92	-0.33	1.00			
	VHI	0.27	-0.03	-0.13	-0.49	0.59	0.38	0.74	1.00		
	FAL	-0.01	0.25	0.29	0.13	0.31	-0.15	0.35	0.24	1.00	
	PPL	-0.38	0.59	0.36	0.36	0.61	-0.52	0.62	0.24	0.63	1.00
Belgium	PCP	1.00									
	LST	-0.60	1.00								
	ET	-0.61	0.61	1.00							
	PET	-0.71	0.78	0.82	1.00						
	NDVI	-0.21	0.67	0.23	0.19	1.00					
	TCI	0.63	-0.84	-0.60	-0.90	-0.31	1.00				
	VCI	-0.29	0.56	0.05	0.08	0.91	-0.28	1.00			
	VHI	0.20	-0.12	-0.40	-0.60	0.59	0.49	0.70	1.00		
	FAL	0.01	-0.29	-0.25	-0.04	-0.31	0.05	-0.18	-0.12	1.00	
	PPL	-0.58	0.57	0.15	0.45	0.43	-0.54	0.59	0.13	0.29	1.00
UK	PCP	1.00									
	LST	-0.17	1.00								
	ET	-0.27	0.73	1.00							
	PET	-0.37	0.73	0.97	1.00						
	NDVI	-0.16	0.67	0.57	0.48	1.00					
	TCI	0.14	-0.94	-0.71	-0.73	-0.60	1.00				
	VCI	-0.30	0.55	0.55	0.48	0.95	-0.48	1.00			
	VHI	-0.18	-0.31	-0.09	-0.19	0.42	0.44	0.58	1.00		
	FAL	-0.55	-0.06	-0.04	0.02	0.00	0.01	0.20	0.21	1.00	
	PPL	-0.86	0.45	0.52	0.58	0.45	-0.40	0.58	0.22	0.46	1.00
France	PCP	1.00									
	LST	-0.61	1.00								
	ET	-0.57	0.72	1.00							
	PET	-0.73	0.86	0.76	1.00						
	NDVI	-0.24	0.53	0.69	0.27	1.00					
	TCI	0.44	-0.88	-0.59	-0.85	-0.24	1.00				
	VCI	-0.27	0.51	0.73	0.31	0.98	-0.25	1.00			
	VHI	0.09	-0.21	0.20	-0.36	0.68	0.52	0.69	1.00		
	FAL	-0.05	-0.19	0.12	0.04	0.00	0.17	0.04	0.16	1.00	
	PPL	-0.31	0.45	0.74	0.45	0.66	-0.39	0.73	0.35	0.36	1.00

Very strong negative (-1.00 to -0.80)	Strong negative (-0.79 to -0.60)	Moderate negative (-0.59 to -0.40)	Weak negative (-0.39 to -0.20)	Very weak negative (-0.19 to -0.01)
Very strong positive (0.80 to 1.00)	Strong positive (0.60 to 0.79)	Moderate positive (0.40 to 0.59)	Weak positive (0.20 to 0.39)	Very weak positive (0.00 to 0.19)

Table 5. Pair-wise correlation coefficients computed for Spain, Switzerland, Italy, Ukraine and Poland.

Country	Data	PCP	LST	ET	PET	NDVI	TCI	VCI	VHI	FAL	PPL
Spain	PCP	1.00									
	LST	-0.75	1.00								
	ET	0.22	-0.29	1.00							
	PET	-0.63	0.77	-0.01	1.00						
	NDVI	0.13	-0.13	0.87	-0.05	1.00					
	TCI	0.22	-0.67	0.25	-0.67	0.24	1.00				
	VCI	0.25	-0.21	0.86	-0.14	0.98	0.24	1.00			
	VHI	0.29	-0.42	0.81	-0.37	0.91	0.58	0.93	1.00		
	FAL	-0.15	0.28	0.38	0.27	0.53	-0.14	0.49	0.36	1.00	
	PPL	-0.11	0.20	0.46	0.46	0.53	-0.14	0.49	0.36	0.67	1.00
Switzerland	PCP	1.00									
	LST	-0.32	1.00								
	ET	-0.52	0.78	1.00							
	PET	-0.65	0.78	0.92	1.00						
	NDVI	-0.12	0.89	0.61	0.54	1.00					
	TCI	0.38	-0.89	-0.79	-0.78	-0.78	1.00				
	VCI	-0.41	0.84	0.67	0.66	0.85	-0.68	1.00			
	VHI	-0.17	0.27	0.13	0.12	0.39	0.06	0.69	1.00		
	FAL	-0.12	0.13	0.32	0.14	0.21	-0.09	0.13	0.09	1.00	
	PPL	-0.18	0.54	0.61	0.35	0.58	-0.59	0.40	-0.04	0.42	1.00
Italy	PCP	1.00									
	LST	-0.69	1.00								
	ET	-0.02	0.03	1.00							
	PET	-0.61	0.68	0.38	1.00						
	NDVI	-0.14	0.27	0.82	0.26	1.00					
	TCI	0.29	-0.73	0.05	-0.63	0.07	1.00				
	VCI	-0.08	0.18	0.91	0.33	0.96	0.06	1.00			
	VHI	0.04	-0.11	0.84	0.06	0.89	0.43	0.93	1.00		
	FAL	-0.10	0.23	0.57	0.27	0.71	-0.03	0.66	0.59	1.00	
	PPL	0.12	0.11	0.64	0.43	0.59	-0.18	0.67	0.54	0.44	1.00
Ukraine	PCP	1.00									
	LST	-0.61	1.00								
	ET	0.20	0.01	1.00							
	PET	-0.31	0.58	-0.02	1.00						
	NDVI	-0.33	0.69	0.08	0.09	1.00					
	TCI	0.42	-0.78	-0.06	-0.79	-0.21	1.00				
	VCI	0.19	0.34	0.06	0.14	0.64	-0.18	1.00			
	VHI	0.49	-0.41	-0.01	-0.56	0.28	0.72	0.56	1.00		
	FAL	0.11	0.23	0.50	0.31	0.13	-0.36	0.20	-0.16	1.00	
	PPL	0.30	-0.50	-0.42	0.00	-0.39	0.31	-0.20	0.12	-0.38	1.00
Poland	PCP	1.00									
	LST	-0.32	1.00								
	ET	-0.09	0.50	1.00							
	PET	-0.32	0.67	0.73	1.00						
	NDVI	-0.20	0.82	0.50	0.42	1.00					
	TCI	0.29	-0.86	-0.49	-0.75	-0.60	1.00				
	VCI	-0.08	0.62	0.59	0.31	0.92	-0.44	1.00			
	VHI	0.11	0.08	0.31	-0.17	0.59	0.20	0.79	1.00		
	FAL	0.14	0.32	0.72	0.45	0.37	-0.30	0.49	0.33	1.00	
	PPL	-0.28	0.08	-0.03	0.05	0.06	-0.02	0.00	-0.01	-0.03	1.00

Very strong negative (-1.00 to -0.80)	Strong negative (-0.79 to -0.60)	Moderate negative (-0.59 to -0.40)	Weak negative (-0.39 to -0.20)	Very weak negative (-0.19 to -0.01)
Very strong positive (0.80 to 1.00)	Strong positive (0.60 to 0.79)	Moderate positive (0.40 to 0.59)	Weak positive (0.20 to 0.39)	Very weak positive (0.00 to 0.19)

3.4. Discussion with previous research

This subsection is dedicated to discussing the findings of the present study in conjunction with the results derived from prior research. As previously noted, the majority of studies investigating the impacts of climate change concentrated on specific regions of the world, with a notable scarcity of research conducted at country scale. This subsection will provide information about these limited country-scale studies, offering an exploration into the unique aspects and insights they bring to the understanding of climate change impacts.

To the best of my knowledge, limited research has explored the consequences of climate change on European countries in the recent years. Salvati et al. [93] discovered a non-uniform decrease in annual rainfall and an increase in the aridity index across Italy between 1951 and 2007. This variability affected various land cover classes, with natural and semi-natural areas proving to be the most susceptible to climate-induced aridity. Their findings offer valuable insights for sustainable regional planning in the context of climate change in the Mediterranean basin. Szewczak et al. [94] observed a declining trend in the climatic water balance across numerous locations in Poland, indicating the widespread emergence of drought conditions throughout the majority of the country. In the case of Romania, Prăvălie et al. [95] reported an overall greening trend in national forests between 1987 and 2018, particularly in the Carpathians region. This suggests enhanced vegetation productivity, especially in high-altitude areas. Simultaneously, many regions across the country experienced concurrent increases in temperature, PCP and ET during the same time frame. Cheval et al. [96] noted an increase in LST in Romania from 2000 to 2018 using MODIS LST data. Furthermore, Cheval et al. [97] combined thermal hazard elements from LST with vulnerability metrics based on PPL density and urban structure. Their findings revealed an elevated urban heat hazard-risk during daytime, in warmer climates and in densely populated cities in Romania.

A comprehensive analysis of the literature indicated that a greater number of studies have examined the effects of climate change on Asian countries compared to those conducted on European countries. Xu et al. [98] noted a significant increase in the mean NDVI in China from 1982 to 2011. They established a strong positive correlation between the time series of annual average NDVI values at the national scale and air temperature, while the correlation with annual PCP was deemed insignificant. Similarly, Piao et al. [99] showcased an augmentation in vegetation greenness in China between 1982 and 2009, utilizing satellite-derived Leaf Area Index datasets and five distinct ecosystem models. Bhattarai et al. [100] observed a rise in PCP and ET in India from 2001 to 2016, while Rasul et al. [101] documented an increase in PCP in Iraq from 1981 to 2019. Cao et al. [102] examined the spatio-temporal distribution of climate potential productivity across China from 1980 to 2018, focusing on the ideal state of natural vegetation without human influence. Their findings indicate that increasing global temperatures and declining PCP significantly impact terrestrial ecosystem productivity, with PCP being the primary factor. The effects vary across different sub-regions and ecosystems, offering insights into how vegetation productivity in China responds to climate change. Mu et al. [103] indicated a consistent enhancement in vegetation growth in China between 2001 and 2018, with the primary driving force being the continuous increase in CO_2 levels. Prodhan et al. [104] estimated the agricultural drought trends in South Asia from 2001 to 2016 using the Mann-Kendall test. They identified spatial and temporal patterns, revealing an increasing drought trend in the central part of Afghanistan and north-western Pakistan during the start and length of the season, as well as in Afghanistan, central Pakistan and north-western India during the end of the season, attributed to erratic rainfall patterns and high PET. Huang et al. [105] used Landsat images and interpolation methods to analyse surface water dynamics in Central Asia from 1990 to 2019 at a 30-m spatial resolution. The results revealed a significant decline in permanent surface water areas in downstream countries with water scarcity, particularly in Kazakhstan. The findings underscore the impact of climatic changes and human activities, such as PPL growth and reservoir areas, on surface water resources, highlighting the intensification of the water crisis in Central Asia and emphasizing the need for sustainable water management strategies to address future challenges. Pradhan et al. [106] revealed that, in the recent years, South Korea's climate has experienced a rise in temperature variability across seasons. There has been a swift decline in the frequency of days experiencing low temperatures, coupled with a concurrent rise in maximum PCP during the summer [106-108].

Too few studies focused on African countries. Tantawi [109] found an increasing trend in annual average temperature in Libya between 1975 and 2000. Additionally, during the period from 1951 to 2000, there was an increasing trend in annual PCP, while a decreasing trend in annual PCP was noted from 1976 to 2000. Furthermore, Libya witnessed a growing trend in annual average humidity from 1951 to 2000. Abera et al. [110] utilized a Budyko-like framework and remote sensing data to assess the impact of climate change and land surface changes on water availability in Ethiopia. On a national scale, the mean long-term annual runoff increased positively by about 80 mm/year over 20 years, with both climate change and landscape surface changes contributing equally (50% each). However, spatial variations were observed, with climate change playing a larger role in water resource changes in northern and south-eastern Ethiopia, particularly in the Somali region, where 70% of the changes were attributed to climate change.

A limited number of studies examined the global impacts of climate change. Mu et al. [111] documented a rise in drought occurrences in the Amazon, western Europe and western Russia regions from 2000 to 2011. In another study, McCabe and Wolock [112] utilized monthly PCP and PET data to calculate monthly PCP minus PET (PMPE) for global land areas. Despite an

increase in global PET and temperature between 1901 and 2009, the study found that the percentage of global land experiencing drought remained unchanged, attributed to a concurrent increase in global PCP mitigating the impact of increased PET on drought conditions.

According to Reiners et al. [3] the relationship between FAL and LST is less evident in the temperate climate zone, where European countries are situated. The current study supports this observation. As seen in Tables 4 and 5, a positive correlation was found between FAL and LST in all countries except for France, Belgium and the UK. Additionally, Fig. 2 illustrates a consistent rise in drought conditions across all countries examined in this study in recent years. This finding does not only align well with the findings of [93-98], who reported an increase in drought conditions in European countries in recent years; but also with the findings of Bhattarai et al. [100], Prodhan et al. [104] and Huang et al. [105], who also reported a surge in drought occurrences in Asian countries in recent years. These findings collectively underscore a global trend of increasing drought conditions, with the current study supporting and extending observations made by previous studies.

4. Conclusion

Investigating the effects of climate change through remote sensing data is crucial as it provides a comprehensive and objective assessment of environmental changes. Remote sensing allows for large-scale monitoring, enabling the identification of patterns and trends in climate-related variables over time. This data-driven approach enhances our understanding of climate dynamics, supports informed decision-making and contributes to effective mitigation and adaptation strategies. Hence, this study aimed to examine the impacts of climate change on European countries Türkiye, Germany, Belgium, the UK, France, Spain, Switzerland, Italy, Ukraine and Poland from 2001 to 2022 using remote sensing data obtained from the GEE catalogues.

The UK experienced the most significant decline in PCP since 2001, while Ukraine and Poland exhibited a higher rate of LST increase compared to other countries. Türkiye and Italy were least affected by LST rise. Switzerland, France and Italy had a higher increase in ET rates, while Belgium, France and Italy experienced the highest rate of PET increase. Türkiye and Poland had a more pronounced rise in NDVI values, indicating healthier vegetation, while Italy and Poland showed the most dramatic increase in VCI values. Switzerland, Belgium and Germany exhibited a higher rate of TCI decrease, indicating the most severe drought conditions. FAL rates were higher in Germany and Spain, with Poland, France and Italy having more moderate increases. Türkiye and the UK experienced the most significant PPL increase among all countries between 2001 and 2023. As for the relationships between the environmental parameters examined, strong positive correlations were noted between LST and ET as well as PET, while LST exhibited a notable correlation with NDVI. PCP generally showed a negative correlation with other factors and ET correlated significantly with NDVI and VCI. Directly linking TCI and FAL with other factors proved challenging, although there was some observable impact of increasing PPL on FAL. It is also difficult to state a direct impact of increasing PPL on climate parameters. It can also be concluded that the results of this study align well with the outcomes of earlier research conducted in European countries.

Time-series analysis of remote sensing data offers a dynamic perspective into the evolving impact of climate change, providing a comprehensive understanding of environmental trends over time. By examining temporal patterns, researchers can discern subtle shifts, track long-term changes and identify anomalies in various climatic parameters. This will give the opportunity to uncover critical insights into the complex interplay of climate variables, allowing for more precise and targeted mitigation strategies. The ability to observe temporal trends facilitates the identification of emerging patterns, aiding in the prediction of potential environmental challenges. Moreover, time-series analysis empowers decision-makers with actionable data, enhancing the formulation of adaptive measures to address the multifaceted effects of climate change on ecosystems and societies. Overall, this method plays a pivotal role in advancing our understanding and response to the evolving dynamics of climate change.

Conflict of interest

The author declares no conflict of interest.

References

1. The Sustainable Development Goals Report 2019. https://sdgs.un.org/goals. (accessed 2 September 2024).
2. Zhao, S., Liu, M., Tao, M., Zhou, W., Lu, X., Xiong, Y., Li, F. & Wang, Q. (2023). The role of satellite remote sensing in mitigating and adapting to global climate change. Science of the Total Environment, 166820.
3. Reiners, P., Sobrino, J., & Kuenzer, C. (2023). Satellite-derived land surface temperature dynamics in the context of global change—A review. Remote Sensing, 15(7), 1857.
4. Kotan, B., Tatmaz, A., Kılıç, S., & Erener, A. (2021). LST change for 16-year period for different land use classes. Advanced Remote Sensing, 1(1), 38-45.
5. Sarp, G., Baydoğan, E., Güzel, F., & Otlukaya, T. (2021). Evaluation of the relationship between urban area and land surface temperature determined from optical satellite data: A case of Istanbul. Advanced Remote Sensing, 1(1), 31-37.
6. Bünyan Ünel, F., Kuşak, L., Yakar, M., Doğan, H. (2023). Coğrafi bilgi sistemleri ve analitik hiyerarşi prosesi kullanarak Mersin ilinde otomatik meteoroloji gözlem istasyonu yer seçimi. Geomatik, 8(2), 107-123. https://doi.org/10.29128/geomatik.1136951.

7. Mogaraju, J. K. (2024). Machine learning assisted prediction of land surface temperature (LST) based on major air pollutants over the Annamayya District of India. International Journal of Engineering and Geosciences, 9(2), 233-246.
8. Morsy, S., & Hadı, M. (2022). Impact of land use/land cover on land surface temperature and its relationship with spectral indices in Dakahlia Governorate, Egypt. International Journal of Engineering and Geosciences, 7(3), 272-282.
9. Guha, S., & Govil, H. (2022). Estimating the seasonal relationship between land surface temperature and normalized difference bareness index using Landsat data series. International Journal of Engineering and Geosciences, 7(1), 9-16.
10. Zheng, C., Jia, L., & Hu, G. (2022). Global land surface evapotranspiration monitoring by ETMonitor model driven by multi-source satellite earth observations. Journal of Hydrology, 613, 128444.
11. Tahsin, A., Abdullahi, J., Karabulut, A. İ., & Yesilnacar, M. İ. (2023). Spatiotemporal prediction of reference evapotranspiration in Araban Region, Türkiye: A machine learning based approach. Advanced Remote Sensing, 3(1), 27-37.
12. Yağcı, A. L. (2023). Bolu Yeniçağa'da evapotranspirasyonun Landsat uydu görüntüleri ve trapezoid model ile izlenmesi. Geomatik, 8(1), 18-26.
13. Kamran, K. V., Sourghali, M., & Bagheri, S. (2024). A comparative spectral assessment approach of SEBAL and SEBS for actual evaporation estimation in Ardabil Province. International Journal of Engineering and Geosciences, 9(2), 131-146.
14. Tabari, H. (2020). Climate change impact on flood and extreme precipitation increases with water availability. Scientific Reports, 10(1), 13768.
15. Cassia, R., Nocioni, M., Correa-Aragunde, N., & Lamattina, L. (2018). Climate change and the impact of greenhouse gasses: CO2 and NO, friends and foes of plant oxidative stress. Frontiers in Plant Science, 9, 273.
16. Zheng, X., Streimikiene, D., Balezentis, T., Mardani, A., Cavallaro, F., & Liao, H. (2019). A review of greenhouse gas emission profiles, dynamics, and climate change mitigation efforts across the key climate change players. Journal of Cleaner Production, 234, 1113-1133.
17. Choudhury, D., Das, K., & Das, A. (2019). Assessment of land use land cover changes and its impact on variations of land surface temperature in Asansol-Durgapur Development Region. The Egyptian Journal of Remote Sensing and Space Science, 22(2), 203-218.
18. Chao, Z., Wang, L., Che, M., & Hou, S. (2020). Effects of different urbanization levels on land surface temperature change: Taking Tokyo and Shanghai for example. Remote Sensing, 12(12), 2022.
19. Rosas-Chavoya, M., López-Serrano, P. M., Vega-Nieva, D. J., Wehenkel, C. A., & Hernández-Díaz, J. C. (2022). Application of Land Surface temperature from Landsat series to monitor and analyze forest ecosystems: A bibliometric analysis. Forest Systems, 31(3), e021-e021.
20. Kumar, A., Agarwal, V., Pal, L., Chandniha, S. K., & Mishra, V. (2021). Effect of land surface temperature on urban heat island in Varanasi City, India. J-Multidisciplinary Scientific Journal, 4(3), 420-429.
21. Ghiat, I., Mackey, H. R., & Al-Ansari, T. (2021). A review of evapotranspiration measurement models, techniques and methods for open and closed agricultural field applications. Water, 13(18), 2523.
22. Ma, S., Eichelmann, E., Wolf, S., Rey-Sanchez, C., & Baldocchi, D. D. (2020). Transpiration and evaporation in a Californian oak-grass savanna: Field measurements and partitioning model results. Agricultural and Forest Meteorology, 295, 108204.
23. Tadese, M., Kumar, L., & Koech, R. (2020). Long-term variability in potential evapotranspiration, water availability and drought under climate change scenarios in the Awash River Basin, Ethiopia. Atmosphere, 11(9), 883.
24. Ajjur, S. B., & Al-Ghamdi, S. G. (2021). Evapotranspiration and water availability response to climate change in the Middle East and North Africa. Climatic Change, 166(3), 28.
25. Zhang, Q., Yang, Z., Hao, X., & Yue, P. (2019). Conversion features of evapotranspiration responding to climate warming in transitional climate regions in northern China. Climate Dynamics, 52, 3891-3903.
26. Um, M. J., Kim, Y., Park, D., Jung, K., Wang, Z., Kim, M. M., & Shin, H. (2020). Impacts of potential evapotranspiration on drought phenomena in different regions and climate zones. Science of the Total Environment, 703, 135590.
27. Felton, A. J., Slette, I. J., Smith, M. D., & Knapp, A. K. (2020). Precipitation amount and event size interact to reduce ecosystem functioning during dry years in a mesic grassland. Global Change Biology, 26(2), 658-668.
28. Agovino, M., Casaccia, M., Ciommi, M., Ferrara, M., & Marchesano, K. (2019). Agriculture, climate change and sustainability: The case of EU-28. Ecological Indicators, 105, 525-543.
29. Rahmani Fazli, A., & Salehian, S. (2022). The effects of Temperature and Precipitation changes on the occurrence of water resources instability in Zayandeh-Rud Basin. Journal of Arid Regions Geographic Studies, 8(29), 52-68.
30. Manabe, S. (2019). Role of greenhouse gas in climate change. Tellus A: Dynamic Meteorology and Oceanography, 71(1), 1620078.

31. Jeffry, L., Ong, M. Y., Nomanbhay, S., Mofijur, M., Mubashir, M., & Show, P. L. (2021). Greenhouse gases utilization: A review. Fuel, 301, 121017.
32. Driga, A. M., & Drigas, A. S. (2019). Climate Change 101: How Everyday Activities Contribute to the Ever-Growing Issue. International Journal of Recent Contributions from Engineering, Science & IT, 7(1), 22-31.
33. Dupuy, J. L., Fargeon, H., Martin-StPaul, N., Pimont, F., Ruffault, J., Guijarro, M., Hernando, C., Madrigal, J., & Fernandes, P. (2020). Climate change impact on future wildfire danger and activity in southern Europe: a review. Annals of Forest Science, 77, 1-24.
34. Yang, J., Gong, P., Fu, R., Zhang, M., Chen, J., Liang, S., Xu, B., Shi, J., & Dickinson, R. (2013). The role of satellite remote sensing in climate change studies. Nature Climate Change, 3(10), 875-883.
35. Kotchi, S. O., Bouchard, C., Ludwig, A., Rees, E. E., & Brazeau, S. (2019). Using Earth observation images to inform risk assessment and mapping of climate change-related infectious diseases. Canada Communicable Disease Report= Releve des Maladies Transmissibles au Canada, 45(5), 133-142.
36. Şenol, H. İ., Kaya, Y., Yiğit, A. Y., & Yakar, M. (2024). Extraction and geospatial analysis of the Hersek Lagoon shoreline with Sentinel-2 satellite data. Survey Review, 56(397), 367-382.
37. Mokhtar, K., Chuah, L. F., Abdullah, M. A., Oloruntobi, O., Ruslan, S. M. M., Albasher, G., Ali, A., & Akhtar, M. S. (2023). Assessing coastal bathymetry and climate change impacts on coastal ecosystems using Landsat 8 and Sentinel-2 satellite imagery. Environmental Research, 239, 117314.
38. Hashim, B. M., Sultan, M. A., Attyia, M. N., Al Maliki, A. A., & Al-Ansari, N. (2019). Change detection and impact of climate changes to Iraqi southern marshes using Landsat 2 MSS, Landsat 8 OLI and Sentinel 2 MSI data and GIS applications. Applied Sciences, 9(10), 2016.
39. Bannari, A., & Al-Ali, Z. M. (2020). Assessing climate change impact on soil salinity dynamics between 1987–2017 in arid landscape using Landsat TM, ETM+ and OLI data. Remote Sensing, 12(17), 2794.
40. Eleftheriou, D., Kiachidis, K., Kalmintzis, G., Kalea, A., Bantasis, C., Koumadoraki, P., Spathara, M. E., Tsolaki, A., Tzampazidou, M. I., & Gemitzi, A. (2018). Determination of annual and seasonal daytime and nighttime trends of MODIS LST over Greece-climate change implications. Science of the Total Environment, 616, 937-947.
41. Jabal, Z. K., Khayyun, T. S., & Alwan, I. A. (2022). Impact of climate change on crops productivity using MODIS-NDVI time series. Civil Engineering Journal, 8(6), 1136-1156.
42. Tian, L., Tao, Y., Fu, W., Li, T., Ren, F., & Li, M. (2022). Dynamic simulation of land use/cover change and assessment of forest ecosystem carbon storage under climate change scenarios in Guangdong Province, China. Remote Sensing, 14(10), 2330.
43. Gruber, A., Scanlon, T., van der Schalie, R., Wagner, W., & Dorigo, W. (2019). Evolution of the ESA CCI Soil Moisture climate data records and their underlying merging methodology. Earth System Science Data, 11(2), 717-739.
44. Qu, C., Hao, X., & Qu, J. J. (2019). Monitoring extreme agricultural drought over the Horn of Africa (HOA) using remote sensing measurements. Remote Sensing, 11(8), 902.
45. Imran, M., & Mehmood, A. (2020). Analysis and mapping of present and future drivers of local urban climate using remote sensing: a case of Lahore, Pakistan. Arabian Journal of Geosciences, 13(6), 278.
46. Wu, L., Ma, X., Dou, X., Zhu, J., & Zhao, C. (2021). Impacts of climate change on vegetation phenology and net primary productivity in arid Central Asia. Science of the Total Environment, 796, 149055.
47. Yi, L., Jing, W., Ke, C., Zhaonan, C. A. I., Dongxu, Y. A. N. G., & Lin, W. U. (2021). Satellite remote sensing of greenhouse gases: Progress and trends. National Remote Sensing Bulletin, 25(1), 53-64.
48. Jiao, W., Wang, L., & McCabe, M. F. (2021). Multi-sensor remote sensing for drought characterization: current status, opportunities and a roadmap for the future. Remote Sensing of Environment, 256, 112313.
49. Shah, P. B., & Patel, C. R. (2023). Integration of Remote Sensing and Big Data to Study Spatial Distribution of Urban Heat Island for Cities with Different Terrain. International Journal of Engineering, 36(1), 71-77.
50. Mpandeli, S., Nhamo, L., Moeletsi, M., Masupha, T., Magidi, J., Tshikolomo, K., Liphadzi, S., Naidoo, D., & Mabhaudhi, T. (2019). Assessing climate change and adaptive capacity at local scale using observed and remotely sensed data. Weather and Climate Extremes, 26, 100240.
51. Javadinejad, S., Eslamian, S., & Ostad-Ali-Askari, K. (2019). Investigation of monthly and seasonal changes of methane gas with respect to climate change using satellite data. Applied Water Science, 9, 1-8.
52. Pádua, L., Marques, P., Adão, T., Guimarães, N., Sousa, A., Peres, E., & Sousa, J. J. (2019). Vineyard variability analysis through UAV-based vigour maps to assess climate change impacts. Agronomy, 9(10), 581.
53. Park, H., Kim, K., & Lee, D. K. (2019). Prediction of severe drought area based on random forest: Using satellite image and topography data. Water, 11(4), 705.
54. Orusa, T., & Borgogno Mondino, E. (2021). Exploring short-term climate change effects on rangelands and broad-leaved forests by free satellite data in Aosta Valley (Northwest Italy). Climate, 9(3), 47.

55. Pareeth, S., & Karimi, P. (2023). Evapotranspiration estimation using Surface Energy Balance Model and medium resolution satellite data: An operational approach for continuous monitoring. Scientific Reports, 13(1), 12026.
56. Climate Change Knowledge Portal, https://climateknowledgeportal.worldbank.org/ (accessed 2 September 2024).
57. Climate of Germany, https://www.britannica.com/place/Germany/Climate (accessed 2 September 2024).
58. Climate of Belgium, https://www.weatheronline.co.uk/reports/climate/Belgium (accessed 2 September 2024).
59. Climate of the UK, https://climateknowledgeportal.worldbank.org/country/united-kingdom (accessed 2 September 2024).
60. Climate of France, https://www.britannica.com/place/France/Climate (accessed 2 September 2024).
61. Climate of Spain, https://www.weatheronline.co.uk/reports/climate/Spain (accessed 2 September 2024).
62. Climate of Switzerland, https://www.britannica.com/place/Switzerland/Relief-and-drainage (accessed 2 September 2024).
63. Climate of Italy, https://www.weatheronline.co.uk/reports/climate/Italy (accessed 2 September 2024).
64. Climate of Ukraine https://www.worlddata.info/europe/ukraine/climate.php (accessed 2 September 2024).
65. Climate of Poland https://www.britannica.com/place/Poland/Climate (accessed 2 September 2024).
66. Funk, C., Peterson, P., Landsfeld, M., Pedreros, D., Verdin, J., Shukla, S., Husak, G., Rowland, J., Harrison, L., Hoell, A., & Michaelsen, J. (2015). The climate hazards infrared precipitation with stations—a new environmental record for monitoring extremes. Scientific Data, 2(1), 1-21.
67. Belay, A. S., Fenta, A. A., Yenehun, A., Nigate, F., Tilahun, S. A., Moges, M. M., Dessie, M., Adgo, E., Nyssen, J., Chen, M., Griensven, A. V., & Walraevens, K. (2019). Evaluation and application of multi-source satellite rainfall product CHIRPS to assess spatio-temporal rainfall variability on data-sparse western margins of Ethiopian highlands. Remote Sensing, 11(22), 2688.
68. CHIRPS Daily: Climate Hazards Center InfraRed Precipitation With Station Data (Version 2.0 Final), https://developers.google.com/earth-engine/datasets/catalog/UCSB-CHG_CHIRPS_DAILY (accessed 2 September 2024).
69. MOD11A1.061 Terra Land Surface Temperature and Emissivity Daily Global 1km, https://developers.google.com/earth-engine/datasets/catalog/MODIS_061_MOD11A1 (accessed 2 September 2024).
70. MOD16A2.061: Terra Net Evapotranspiration 8-Day Global 500m, https://developers.google.com/earth-engine/datasets/catalog/MODIS_061_MOD16A2 (accessed 2 September 2024).
71. MOD13Q1.061 Terra Vegetation Indices 16-Day Global 250m, https://developers.google.com/earth-engine/datasets/catalog/MODIS_061_MOD13Q1 (accessed 2 September 2024).
72. Jiao, W., Zhang, L., Chang, Q., Fu, D., Cen, Y., & Tong, Q. (2016). Evaluating an enhanced vegetation condition index (VCI) based on VIUPD for drought monitoring in the continental United States. Remote Sensing, 8(3), 224.
73. Kogan, F. N. (1990). Remote sensing of weather impacts on vegetation in non-homogeneous areas. International Journal of Remote Sensing, 11(8), 1405-1419.
74. Liang, L., Sun, Q., Luo, X., Wang, J., Zhang, L., Deng, M., Di, L., & Liu, Z. (2017). Long-term spatial and temporal variations of vegetative drought based on vegetation condition index in China. Ecosphere, 8(8), e01919.
75. Zhou, X., Wang, P., Tansey, K., Zhang, S., Li, H., & Wang, L. (2020). Developing a fused vegetation temperature condition index for drought monitoring at field scales using Sentinel-2 and MODIS imagery. Computers and Electronics in Agriculture, 168, 105144.
76. Patel, N. R., Mukund, A., & Parida, B. R. (2022). Satellite-derived vegetation temperature condition index to infer root zone soil moisture in semi-arid province of Rajasthan, India. Geocarto International, 37(1), 179-195.
77. Behifar, M., Kakroodi, A. A., Kiavarz, M., & Azizi, G. (2023). Satellite-based drought monitoring using optimal indices for diverse climates and land types. Ecological Informatics, 76, 102143.
78. Zhang, Y., Wang, P., Tansey, K., Li, M., Guo, F., Liu, J., & Zhang, S. (2023). Spatiotemporal Data Fusion of Index-Based VTCI Using Sentinel-2 and-3 Satellite Data for Field-Scale Drought Monitoring. IEEE Transactions on Geoscience and Remote Sensing, 62, 1-15.
79. Kogan, F. N. (1995). Application of vegetation index and brightness temperature for drought detection. Advances in Space Research, 15(11), 91-100.
80. Bento, V. A., Gouveia, C. M., DaCamara, C. C., Libonati, R., & Trigo, I. F. (2020). The roles of NDVI and Land Surface Temperature when using the Vegetation Health Index over dry regions. Global and Planetary Change, 190, 103198.
81. Kogan, F. N. (2000). Satellite-observed sensitivity of world land ecosystems to El

Nino/La Nina. Remote Sensing of Environment, 74(3), 445-462.
82. Karnieli, A., Agam, N., Pinker, R. T., Anderson, M., Imhoff, M. L., Gutman, G. G., Panov, N., & Goldberg, A. (2010). Use of NDVI and land surface temperature for drought assessment: Merits and limitations. Journal of Climate, 23(3), 618-633.
83. Hansen, M. C., Potapov, P. V., Moore, R., Hancher, M., Turubanova, S. A., Tyukavina, A., Thau, D., Stehman, S. V., Goetz, S. J., Loveland, T. R., Kommareddy, A., Egorov, A., Chini, L., Justice, C. O., & Townshend, J. R. (2013). High-resolution global maps of 21st-century forest cover change. Science, 342(6160), 850-853.
84. Hansen Global Forest Change v1.11 (2000-2023), https://developers.google.com/earth-engine/datasets/catalog/UMD_hansen_global_forest_change_2023_v1_11 (accessed 2 September 2024).
85. Shimizu, K., Ota, T., & Mizoue, N. (2020). Accuracy assessments of local and global forest change data to estimate annual disturbances in temperate forests. Remote Sensing, 12(15), 2438.
86. Macrotrends - The Premier Research Platform for Long Term Investors, https://www.macrotrends.net/ (accessed 2 September 2024).
87. Turkish Statistical Institute, https://www.tuik.gov.tr/ (accessed 2 September 2024).
88. Mann, H. B. (1945). Nonparametric tests against trend. Econometrica: Journal of the Econometric Society, 245-259.
89. Kendall, M. G. (1975). Rank Correlation Methods. Griffin, London, UK.
90. Danneberg, J. (2012). Changes in runoff time series in Thuringia, Germany–Mann-Kendall trend test and extreme value analysis. Advances in Geosciences, 31, 49-56.
91. Ullah, W., Ahmad, K., Ullah, S., Tahir, A. A., Javed, M. F., Nazir, A., Abbasi, A. M., Aziz, M., & Mohamed, A. (2023). Analysis of the relationship among land surface temperature (LST), land use land cover (LULC), and normalized difference vegetation index (NDVI) with topographic elements in the lower Himalayan region. Heliyon, 9(2).
92. Fayshal, M. A. (2024). Simulating Land Cover Changes and It's Impacts on Land Surface Temperature: A Case Study in Rajshahi, Bangladesh. Bs.C Thesis, Khulna University of Engineering & Technology.
93. Salvati, L., Sateriano, A., & Zitti, M. (2013). Long-term land cover changes and climate variations–A country-scale approach for a new policy target. Land Use Policy, 30(1), 401-407.
94. Szewczak, K., Łoś, H., Pudełko, R., Doroszewski, A., Gluba, Ł., Łukowski, M., Rafalska-Przysucha, A., Słomiński, J., & Usowicz, B. (2020). Agricultural drought monitoring by MODIS potential evapotranspiration remote sensing data application. Remote Sensing, 12(20), 3411.
95. Prăvălie, R., Sîrodoev, I., Nita, I. A., Patriche, C., Dumitraşcu, M., Roşca, B., Tişcovschi, A., Bandoc, G., Săvulescu, I., Mănoiu, V., & Birsan, M. V. (2022). NDVI-based ecological dynamics of forest vegetation and its relationship to climate change in Romania during 1987–2018. Ecological Indicators, 136, 108629.
96. Cheval, S., Dumitrescu, A., Irașoc, A., Paraschiv, M. G., Perry, M., & Ghent, D. (2022). MODIS-based climatology of the Surface Urban Heat Island at country scale (Romania). Urban Climate, 41, 101056.
97. Cheval, S., Dumitrescu, A., Amihăesei, V., Irașoc, A., Paraschiv, M. G., & Ghent, D. (2023). A country scale assessment of the heat hazard-risk in urban areas. Building and Environment, 229, 109892.
98. Xu, G., Zhang, H., Chen, B., Zhang, H., Innes, J. L., Wang, G., Yan, J., Zheng, Y., Zhu, Z., & Myneni, R. B. (2014). Changes in vegetation growth dynamics and relations with climate over China's landmass from 1982 to 2011. Remote Sensing, 6(4), 3263-3283.
99. Piao, S., Yin, G., Tan, J., Cheng, L., Huang, M., Li, Y., Liu, R., Mao, J., Myneni, R. B., Peng, S., Poulter, B., Shi, X., Xiao, Z., Zeng, N., Zheng, Z., & Wang, Y. (2015). Detection and attribution of vegetation greening trend in China over the last 30 years. Global Change Biology, 21(4), 1601-1609.
100. Bhattarai, N., Mallick, K., Stuart, J., Vishwakarma, B. D., Niraula, R., Sen, S., & Jain, M. (2019). An automated multi-model evapotranspiration mapping framework using remotely sensed and reanalysis data. Remote Sensing of Environment, 229, 69-92.
101. Rasul, A. O., Hameed, H. M., & Ibrahim, G. R. F. (2021). Dramatically increase of built-up area in Iraq during the last four decades. Advanced Remote Sensing, 1(1), 1-9.
102. Ünel, F. B., Kuşak, L., Yakar, M., & Doğan, H. (2023). Coğrafi bilgi sistemleri ve analitik hiyerarşi prosesi kullanarak Mersin ilinde otomatik meteoroloji gözlem istasyonu yer seçimi. *Geomatik*, *8*(2), 107-123.
103. Mu, B., Zhao, X., Wu, D., Wang, X., Zhao, J., Wang, H., Zhou, Q., Du, X., & Liu, N. (2021). Vegetation cover change and its attribution in China from 2001 to 2018. Remote Sensing, 13(3), 496.
104. Prodhan, F. A., Zhang, J., Yao, F., Shi, L., Pangali Sharma, T. P., Zhang, D., Cao, D., Zheng, M., Ahmed, N., & Mohana, H. P. (2021). Deep learning for monitoring agricultural drought in South Asia using remote sensing data. Remote Sensing, 13(9), 1715.
105. Huang, W., Duan, W., & Chen, Y. (2021). Rapidly declining surface and terrestrial water resources in Central Asia driven by socio-economic and climatic changes. Science of the Total Environment, 784, 147193.
106. Pradhan, B., Yoon, S., & Lee, S. (2024). Examining the dynamics of vegetation in South Korea: an

integrated analysis using remote sensing and in situ data. Remote Sensing, 16(2), 300.
107. Kim GangSun, K. G., Lim ChulHee, L. C., Kim SeaJin, K. S., Lee JongYeol, L. J., Son YowHan, S. Y., & Lee WooKyun, L. W. (2017). Effect of national-scale afforestation on forest water supply and soil loss in South Korea, 1971-2010. Sustainability, 9(6), 1-18.
108. Choi, S. W., Kong, W. S., Hwang, G. Y., & Koo, K. A. (2021). Trends in the effects of climate change on terrestrial ecosystems in the Republic of Korea. Journal of Ecology and Environment, 45(1), 13.
109. Tantawi, A. M. M. E. (2005). Climate change in Libya and desertification of Jifara Plain: using geographical information system and remote sensing techniques. Doctoral Thesis, Johannes Gutenberg-Universität Mainz.
110. Abera, W., Tamene, L., Abegaz, A., & Solomon, D. (2019). Understanding climate and land surface changes impact on water resources using Budyko framework and remote sensing data in Ethiopia. Journal of Arid Environments, 167, 56-64.
111. Mu, Q., Zhao, M., Kimball, J. S., McDowell, N. G., & Running, S. W. (2013). A remotely sensed global terrestrial drought severity index. Bulletin of the American Meteorological Society, 94(1), 83-98.
112. McCabe, G. J., & Wolock, D. M. (2015). Variability and trends in global drought. Earth and Space Science, 2(6), 223-228.